

## High-Performance All-Bio-Based Laminates Derived from Delignified Wood

Frey, Marion; Schneider, Livia; Razi, Hajar; Trachsel, Etienne; Faude, Eric; Koch, Sophie Marie; Masania, Kunal; Fratzl, Peter; Keplinger, Tobias; Burgert, Ingo

**DOI**

[10.1021/acssuschemeng.0c08373](https://doi.org/10.1021/acssuschemeng.0c08373)

**Publication date**

2021

**Document Version**

Final published version

**Published in**

ACS Sustainable Chemistry and Engineering

**Citation (APA)**

Frey, M., Schneider, L., Razi, H., Trachsel, E., Faude, E., Koch, S. M., Masania, K., Fratzl, P., Keplinger, T., & Burgert, I. (2021). High-Performance All-Bio-Based Laminates Derived from Delignified Wood. *ACS Sustainable Chemistry and Engineering*, 9(29), 9638-9646.  
<https://doi.org/10.1021/acssuschemeng.0c08373>

**Important note**

To cite this publication, please use the final published version (if applicable).  
Please check the document version above.

**Copyright**

Other than for strictly personal use, it is not permitted to download, forward or distribute the text or part of it, without the consent of the author(s) and/or copyright holder(s), unless the work is under an open content license such as Creative Commons.

**Takedown policy**

Please contact us and provide details if you believe this document breaches copyrights.  
We will remove access to the work immediately and investigate your claim.

# High-Performance All-Bio-Based Laminates Derived from Delignified Wood

Marion Frey,\* Livia Schneider, Hajar Razi, Etienne Trachsel, Eric Faude, Sophie Marie Koch, Kunal Masania, Peter Fratzl, Tobias Keplinger,\* and Ingo Burgert



Cite This: *ACS Sustainable Chem. Eng.* 2021, 9, 9638–9646



Read Online

ACCESS |



Metrics & More



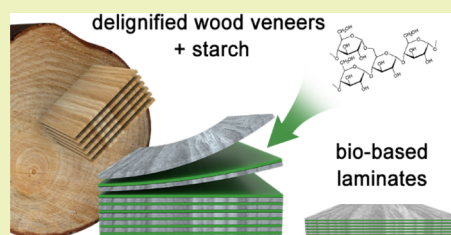
Article Recommendations



Supporting Information

**ABSTRACT:** The need for renewable bio-based materials that could replace well-established synthetic composite materials is rapidly growing. For example, bio-based materials are increasingly used in applications where a lightweight design should be combined with sustainability and recyclability. However, it is often very challenging to directly transfer the excellent properties of biological materials to a product in a scalable and cost-efficient manner. In this study, we combined delignified wood layers (veneers) and a starch-based glue into bio-based high-performance composites. First, we investigated the ideal amount of starch-based glue between the layers to prevent delamination in the final composite. Then, we produced laminates in unidirectional, cross-ply, and quasi-isotropic configurations using wet processing. Laminates with tensile properties up to 40 GPa and 200 MPa in tensile stiffness and strength, respectively, were fabricated with a very high fiber volume content of up to 80%. The high fiber volume contents led to mechanical interlocks between neighboring fibers and made the need for an additional matrix unnecessary. The water-based laminate process is cost-efficient and scalable and additionally allows one to make full use of delignified wood's formability by producing shaped parts for various applications.

**KEYWORDS:** delignified wood, natural fiber composite, all bio-based material, starch adhesive, cellulose



## INTRODUCTION

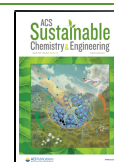
As a result of growing environmental awareness, requirements for new advanced materials in industries, such as the mobility sector, are increasingly considering sustainability aspects and recyclability<sup>1–4</sup> along with low cost, ease of production, and high performance. Hence, plant-derived polymeric materials are at the forefront of today's material development. Fabrication routes for renewable polymer composites generally comprise the synthesis of polymers from plant-based monomers or the direct utilization of polymers extracted from plants, such as cellulose, hemicelluloses, and starch.<sup>5,6</sup> The latter additionally benefits from a favorable energy balance due to the saved energy consumption that is typically needed for polymer synthesis.<sup>7</sup> A very promising and frequently used natural polymer for sustainable composites is cellulose, a polysaccharide composed of a linear chain of  $\beta(1 \rightarrow 4)$ -linked D-glucose units with excellent mechanical properties.<sup>8,9</sup> Inter- and intrachain hydrogen bonding links the individual cellulose chains,<sup>10</sup> which transfers the mechanical properties from the individual polymer chain to the fiber level.<sup>11,12</sup> However, the final transfer of cellulose fiber properties to the macro level in composite applications remains challenging. Limited fiber alignment in the loading direction, relatively low fiber volume contents (FVCs), and a lack of sufficient stress transfer often restrict the full exploitation of cellulose's excellent properties.<sup>13,14</sup>

Well-known effective mechanisms to improve cellulose-fiber-based materials' mechanical properties, for example, in paper,<sup>15</sup> include a distinct fiber interface modification that enhances mechanical interlocking and/or increase bonding strength between fibers. In this regard, fiber–surface fibrillation,<sup>16,17</sup> microfibrillated cellulose addition,<sup>18</sup> or water-soluble hydrophilic dry-strength additives such as starch<sup>19,20</sup> proved highly successful in increasing the bonding area and therefore the bonding strength. Among various studies, Shivryari et al. profited from cellulose nanofibrils' (CNFs) large surface area in paper/nanocellulose laminates. The CNF glue resulted in excellent bonding, and the materials' mechanical properties were able to compete with short glass-fiber-reinforced composites.<sup>21</sup> Recently, Cottonid, a cellulose-based polymer originally developed in 1844 has gained interest as a high-performance cellulosic material. For Cottonid, chemical etching of paper layers prior to lamination results in more accessible OH-groups, which boosts interfiber hydrogen bonding and leads to improved mechanical performance as compared to paper. However, the mechanical properties of

**Received:** November 16, 2020

**Revised:** June 22, 2021

**Published:** July 12, 2021



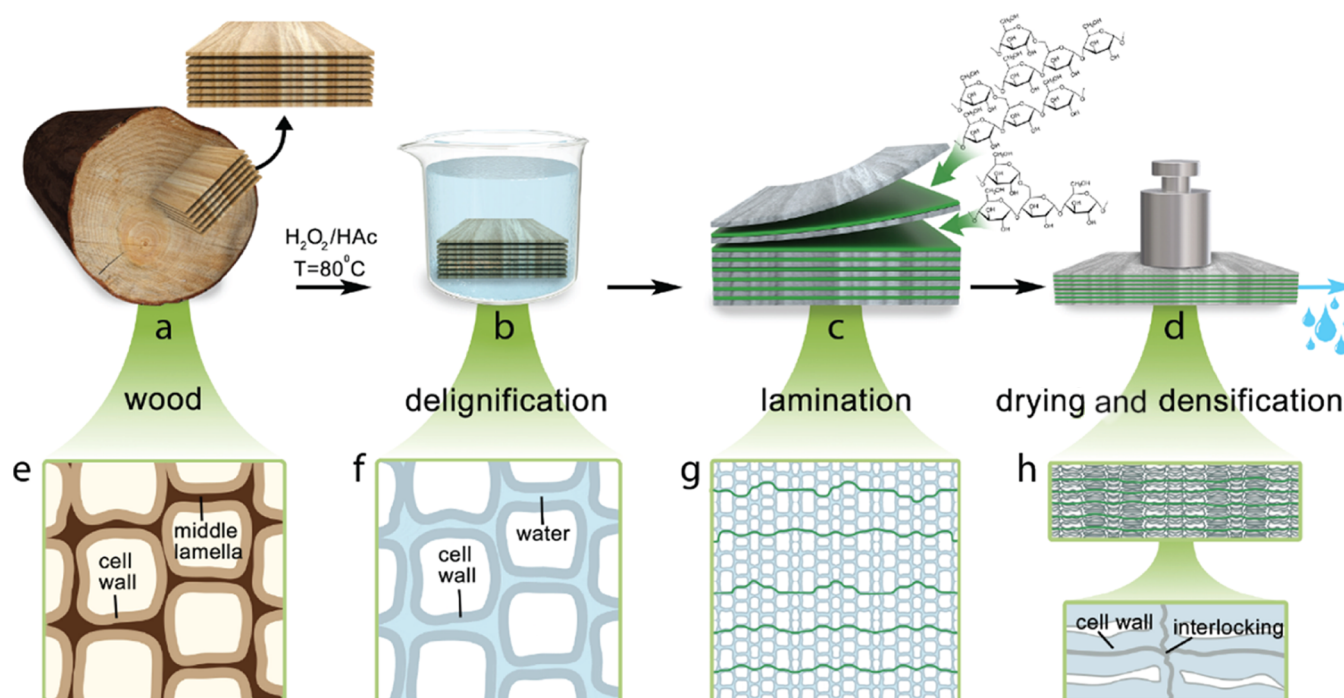


**Figure 1.** (a–d) Starch–cellulose laminate manufacturing procedure and (e–h) the corresponding microstructure of the wood-based material. (a,e) Wood veneers are (b) delignified and washed, which leads to (f) flexible delignified wood veneers due to the free water between the cells. (c) Delignified wood veneers are stacked on top of each other and starch is applied as glue in-between the layers resulting in a wet cellulose–starch laminate (g). (d) Laminate is densified and dried by open mold vacuum-processing leading to (h) densified delignified wood–starch laminates.

paper-based materials such as Cottonid are still limited<sup>22</sup> due to the random orientation of the reinforcing cellulose fibers. Matching the fiber orientation with the loading direction is a common concept exploited in natural materials to make optimal use of their resources.<sup>23,24</sup> In this regard, structure-retaining delignification of wood for cellulose-based materials has proved to be highly successful.<sup>25–28</sup> Unlike in paper making, this top-down process does not distort the fiber alignment and results in a hierarchical, directional cellulose scaffold. Subsequent densification enables achieving very high FVCs of up to 80%, which in combination with mechanical interlocking and intermolecular interactions between neighboring fibers can provide very high tensile stiffness and strength.<sup>29</sup> Despite the material's advantageous properties, the underlying bulk-wood approaches remain challenging, demonstrating the need for scalable laminate processing techniques by stacking and bonding of individual layers.

Here, we combined traditional strategies for fiber–fiber bonding improvement, inspired from paper production, such as mechanical interlocking and starch bonding, with the unidirectional alignment of delignified wood. The presented laminating technique is readily scalable and allows for tunable in-plane properties by using the directional stacking of the delignified wood and densifying to high FVCs (Figure 1). We measured the tensile properties of manufactured laminates and compared the experimental values to data predicted using the classical laminate theory (CLT). By applying an elasto-plastic damage finite element model (FEM), further insights into the fracture behavior were revealed.

## EXPERIMENTAL SECTION

**Delignification.** Norway spruce (*Picea abies*) radial-cut veneers with a density of 0.366 g/cm<sup>3</sup> were cut to the dimensions 150 × 150 × 1.38 mm<sup>3</sup> (1 × r × t). In addition, veneers with the same dimensions

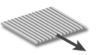
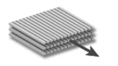
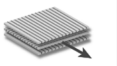
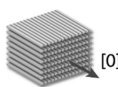
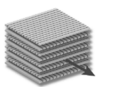
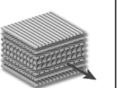
but with a 45° fiber orientation were prepared. Veneers were delignified for 6 h, following the protocol established by Frey et al.<sup>30</sup> For this, 12–15 veneers were separated by metal meshes and were stacked on top of a stainless-steel sample holder in a crystallizing dish (230 mm Ø). A 1:1 volume mixture of glacial acetic acid (VWR Chemicals) and hydrogen peroxide (30 wt %, VWR Chemicals) was poured into the dish until the veneers were fully covered. Samples were then soaked in the solution at RT overnight while stirring at 150 rpm. After this, the solution was heated to 80 °C and the setup was covered with aluminum foil to reduce evaporation. To achieve full delignification, the reaction was conducted for 6 h. Then, veneers were washed with deionized water twice a day until the pH value of the washing water was above 5. The lignin removal was confirmed by IR-spectroscopy (Figure S2) and wet chemistry (Table S4).

**Sample Preparation for Bonding Strength Evaluation.** Collabond 8017 IQ (Agrana Stärke GmbH), a commercial bio-based and biodegradable paper bag adhesive based on modified corn starch, was used as an adhesive between delignified veneers. The product data sheet is available at: [https://www.agrana.com/fileadmin/inhalte/austria/products/2013\\_A4\\_klebstoff\\_web.pdf](https://www.agrana.com/fileadmin/inhalte/austria/products/2013_A4_klebstoff_web.pdf).

The ideal adhesive amount was investigated by the following process. The samples consisted of two delignified wood veneers (90 × 150 mm<sup>2</sup>, radial × longitudinal) that were glued together with an overlap of 30 mm in wet conditions. Prior to gluing, the free water on the veneer surface, which could affect the adhesive concentration, was wiped off with a towel. A 16.5 wt % starch solution (ideal adhesive concentration recommended by the producer) was applied to the overlap (30 × 90 mm<sup>2</sup>) and the applied amount was varied from 0.25, 0.5, and 1.0 to 2.4 g, which correspond to 0.009, 0.019, 0.037, and 0.089 g/cm<sup>2</sup>, respectively. The samples were then densified and dried in the vacuum bag during 3 h at 65 °C as described in the subchapter.

**Bonding Strength Evaluation.** Samples were cut into 20 mm wide stripes and the area that was clamped into the test grips was protected with an adhesive tape. Testing was performed at 20 °C and 65% relative humidity on a universal testing machine (Zwick Roell, 10 kN) with a speed of 1 mm/min. The distance between the clamps

Table 1. Overview of the Seven Different Laminate Lay-Ups Consisting of One, Three, and Eight plies

1-ply	3-ply		8-ply		
					
uni-directional [0]	uni-directional [0/0/0]	cross-ply [0/90/0]	uni-directional [0] [90]	cross-ply [(0/90)2]s	quasi-isotropic [0/90/±45]s

was 90 mm, and the displacement was measured with a clip-on extensometer with an initial distance of 25 mm.

**Laminate Manufacturing.** For laminate manufacturing, wet delignified veneers were stacked on top of one another and starch (370 g/m<sup>2</sup>) was applied between the layers. The fiber orientation of individual layers was chosen in order to obtain the different unidirectional, cross-ply, and quasi-isotropic laminates. Table 1 provides an overview of the one-ply, three-ply, and eight-ply samples that were produced.

**Densification and Drying with the Open-Mold Vacuum Process.** Wet laminates were densified and dried via open-mold vacuum processing. This process allows a simultaneous densification and drying.<sup>30</sup> The wet laminates were placed between two flat, porous, 3D-printed ABS molds and peel ply was applied between the mold and the laminate to protect the molds from contamination. A flow mesh allowed water to flow from the molds to the vacuum tubing, and a spiral tube connected to the vacuum pump surrounded the setup to improve drying. The setup was covered by a vacuum bag and was then placed into an oven at 65 °C and vacuum in the range of 10<sup>−2</sup> mbar was applied according to Frey et al. 2019.<sup>30</sup> One-ply and three-ply laminates were dried and densified for 4.5 h and eight-ply laminates were dried for approximately 30 h.

**Ultramicrotome Cutting and Microscopy.** Cross sections of the eight-ply laminates were analyzed by light microscopy (Olympus BX51) after polishing the cross-sectional surface using an ultramicrotome (Reichert-Jung Ultracut) with a diamond knife. Scanning electron microscopy (SEM) of ruptured surfaces was conducted with a Hitachi SU5000 after applying a Pt–Pd (80/20) coating of 6 nm thickness with a sputter-coater (CCU-010, Safematic).

**Calculation of the FVC.** The FVC of one-ply materials was calculated by dividing its density by the density of cellulose  $\rho_c$ , which was assumed to be 1.5 g/cm<sup>3</sup>. It should be noted that we do not account here for the slightly lower density of the remaining hemicelluloses.

$$\text{FVC} = \frac{\rho}{\rho_c} \quad (1)$$

For the calculation of the fiber–laminate density  $\rho_f$  for three- and eight-ply laminates, the mass of the adhesive starch  $m_s$  needs to be subtracted from the mass of the laminate (eq 2). The starch mass is calculated by the area of the sample times the weight of starch per area (eq 3)

$$\rho_f = \frac{m - m_s}{h \cdot w \cdot l} \quad (2)$$

$$m_s = A \cdot p \quad (3)$$

We applied  $3.69 \times 10^{-4}$  g/mm<sup>2</sup> of 16.5 wt % starch solution in between two delignified wood layers, which corresponds to 0.61 g/mm<sup>2</sup>. Therefore, the amount of adhesive is  $1.22 \times 10^{-4}$  g/mm<sup>2</sup> for three-ply laminates (two adhesive layers) and  $4.26 \times 10^{-4}$  g/mm<sup>2</sup> for eight-ply laminates (seven adhesive layers).

**Tensile Specimen Preparation and Testing.** Laminates were cut into 120 × 20 mm<sup>2</sup> stripes. The clamping area of the samples was reinforced to reduce stress concentrations. One-ply samples were reinforced with masking tape and laminates were reinforced with wood pieces (35 × 20 × 3 mm<sup>3</sup>). The wood pieces and the clamp area

of the laminates were ground to roughen the surface before gluing with a two-component epoxy (Scotch weld DP 460). Before tensile testing, samples were conditioned at 65% RH and 20 °C. Testing was conducted on a universal testing machine (ZwickRoell, Germany) equipped with a 100 kN load cell. The initial testing length was 65 mm and a contact extensometer (ZwickRoell) with an initial length of 25 mm was used to measure the elongation during testing.

**Model Based on CLT.** The behavior of a single ply at 80% FVC in all directions ranging from 0 to 90° was modeled to investigate the influence of the fiber orientation on stiffness (see the Supporting Information). For this calculation, the average 0 and 90° tensile stiffness values of the eight-ply unidirectional laminate, namely, 37.8 and 4.5 GPa, were chosen as approximate values for a one-ply at comparable FVC. We made use of the directionality influence on mechanical properties and created three-ply and eight-ply laminates with tailored in-plane properties and compared the experimentally measured tensile properties with CLT model calculations. By stacking plies at defined angles, we produced eight-ply laminates with unidirectional, cross-ply, and quasi-isotropic lay-ups.

**Finite Element Model.** We studied the elastic properties as well as damage and crack propagation within the composites using an elasto-plastic damage finite element model. The mode was defined by an anisotropic stiffness matrix, anisotropic yield stresses, an equivalent plastic strain ( $\bar{\epsilon}_{p0}^{\text{pl}}$ ) controlling the damage initiation, and a specific fracture energy ( $\Gamma$ ) defining the damage evolution. Models of eight-ply laminates, that is, UD [0], UD [90], QI, and CP, were developed using the finite element program Abaqus (Dassault Systèmes, Johnston, RI). The model geometry was set to replicate the experimental setup (each ply: thickness = 0.25 mm in 120(L) × 20(W) mm<sup>2</sup>, Figure S1). Elastic material models were defined as composite lay-ups of 0, 45, and 90°, in which data for 0 and 90° were taken from the experimental data and 45° was calculated using the composite laminate theory (CLT, Figure 3c). Yield stresses were taken from the experimental data (Figure 4b) and damage properties ( $\bar{\epsilon}_{p0}^{\text{pl}}$ ,  $\Gamma$ ) were assumed to establish a brittle fracture after reaching the yield point. Starch was calculated to yield at 30 MPa and the elastic material properties varied in the model between 3 and 36 GPa yielding at 30 MPa. The upper value was chosen to evaluate the impact of an extreme case.

## RESULTS AND DISCUSSION

Laminating processes including our cellulose-based material necessitate suitable adhesives between layers to avoid delamination. In order to maintain the renewable characteristics of our cellulose-based material, we used a bio-based adhesive mainly consisting of starch. Starch-based glues are well known as bonding agents in papermaking, and adhesives in corrugated boards and play a major role in many other cellulose-based products because they provide good bonding between the cellulose fibers at low cost.<sup>31</sup> One of the major parameters that governs the laminate's final properties is the correct adhesive amount.<sup>32</sup> First, to determine the ideal starch glue amount, we performed mechanical testing on reference samples (no starch) and on samples with varying amounts of starch glue ranging from 90 g/m<sup>2</sup> to 890 g/m<sup>2</sup>. The reference



without starch showed a notable veneer bonding strength of 1.2 MPa (Figure 2a), attributed to a combination of several

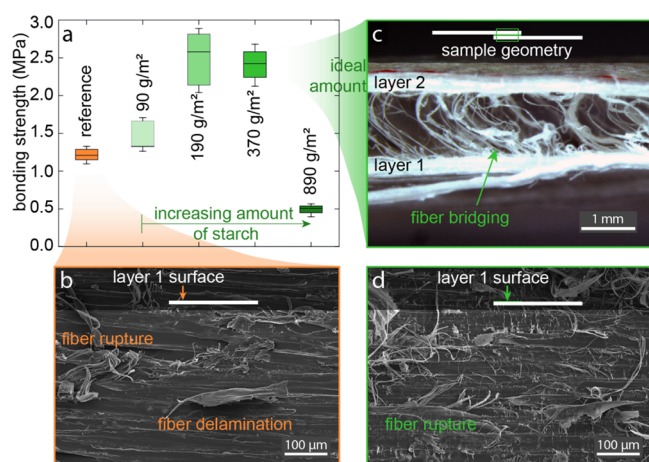


**Figure 2.** (a) Veneer bonding strength of a reference sample (orange) without starch and four different starch concentrations. (b) SEM images of the ruptured surface after bonding strength testing of the reference without starch. (c) Light microscopy image of a bonded veneer sample after failure with an adhesive amount of 370 g/m<sup>2</sup>. (d) SEM image of the ruptured surface after testing of a sample with an adhesive amount of 370 g/m<sup>2</sup>.

mechanisms comprising hydrogen bonding interactions, van der Waals forces, and mechanical interlocking in analogy to the prevailing adhesion mechanisms in paper.<sup>15,20,33</sup> Capillary forces that occur upon drying in combination with the cell wall deformability in the wet state<sup>34</sup> increase the contact area between the two layers. This improves molecular interaction<sup>33</sup> and finally leads to bonding between delignified wood layers even without the use of an adhesive. After failure, SEM images of the bonded area revealed some delaminated fibers and fiber rupturing (Figure 2b). Still, a more homogeneous spread of these defects across the entire gluing area is desired, as this would indicate a larger effective surface area involved in bonding, which could possibly be achieved using a starch-based glue.

The maximum bonding strength increased up to 2.4 MPa by the addition of 370 g/m<sup>2</sup> glue, which is double the strength of the reference sample. Hence, this sample was further analyzed by microscopy techniques. The strong bonding between the layers prevents crack propagation at the interface and thus, it required more energy for the crack to propagate as proven by the light microscopy image of a sample after failure (Figure 2c). The sample exhibited unbroken fibers but also fiber fragments that bridge the existing crack, which increased the crack resistance and energy dissipation at the interface. Starch increased the interfiber bond strength because it compensates the roughness between the fibers and provides OH groups that interact via H-bonding with the delignified wood fibers' OH groups.<sup>17</sup> The SEM image shown in Figure 2d reveals many small fiber fragments that spread out across the whole gluing area, indicating a more homogeneous bonding at the layer–layer interface compared to the reference sample.

When the starch amount exceeded a critical value, the lap shear force decreased drastically even below the reference values. The thick starch layer hindered direct interactions between the layers and did not act as a long-range strong adhesive. A starch amount of 370 g/m<sup>2</sup> was chosen to be

applied between the layers for laminate production because it resulted in a high shear strength and in a relatively low standard deviation compared to other starch amounts.

Utilizing the most suitable interlayer starch amount, we manufactured unidirectional three-ply and eight-ply laminates by alternately stacking delignified wood veneers and starch glue followed by densification. Figure 3a shows that with increasing number of plies, the thickness decreases from 29.4% for a single ply to 19.1% of the initial thickness for eight plies. This corresponds to an increase in FVC from 60% for a single ply up to 80% for eight-ply laminates. These differences in densification at the same pressure level allowed us to investigate the influence of the fiber volume content on tensile properties. Figure 3b illustrates that tensile stiffness increases linearly the higher the FVC is. The increase is in accordance to the upper limit rule of mixtures (ROMs) under the assumption of a single delignified wood fiber stiffness of 50 GPa and confirms the results of our previous study.<sup>35</sup>

We further used CLT to estimate the in-plane stiffness as a function of the ply angle using mechanical properties of the single layers. To apply CLT, interfaces between layers were assumed to be straight and tightly bonded. However, experimentally, these parameters can deviate substantially from this ideal scenario. To gain deeper insights into interfaces between layers, light microscopy investigations of the laminates were performed. Cross sections (Figure 3d–f) indicate that the most prevalent difference among the three laminate types was found in the interface waviness. The unidirectional laminate (Figure 3d) presented a distinct waviness, whereas a cross-ply laminate (Figure 3e) showed straight interfaces and the quasi-isotropic interfaces appeared to be wavy (Figure 3f) but not as pronounced as the unidirectional laminates. This interfacial waviness originates from natural inhomogeneities in wood density, namely, earlywood and latewood. Earlywood consists of thin-walled cells that are highly densified during processing, whereas thicker cell walls (latewood) experience a lower amount of densification at the same force.<sup>35</sup> When radial delignified wood veneers were stacked and densified, stiff latewood regions pressed into the earlywood regions of adjacent layers. This phenomenon was very pronounced in the unidirectional laminate because high-density and low-density regions of individual plies were arranged in parallel to those of neighboring plies and thus enabling a high degree of nesting between adjacent layers. For cross-ply laminates, stiff latewood areas of adjacent layers were arranged in a crosswise manner and were thus not able to nest to the same extent. A decreased variation between plies as found in the quasi-isotropic laminates seems to be sufficient to enable some degree of nesting, though far less than the unidirectional laminates.

This interpenetration of latewood and earlywood regions of adjacent layers may explain the stronger densification of eight-ply unidirectional laminates compared to one-ply and three-ply laminates. It may be concluded that natural density variations were balanced better in eight-ply laminates, simply due to the more available interfaces.

To measure the in-plane tensile stiffness and strength of different lay-up strategies, we tested seven different configurations that are illustrated in Figure 4a. Unidirectional laminates increased linearly to a stiffness in the range 29 and 37 GPa (Figure 4b) with increasing FVC. Unidirectional eight-ply laminates possessed a transverse (90°) stiffness of 4.5 GPa and corresponding strength of 16.9 MPa, respectively. The

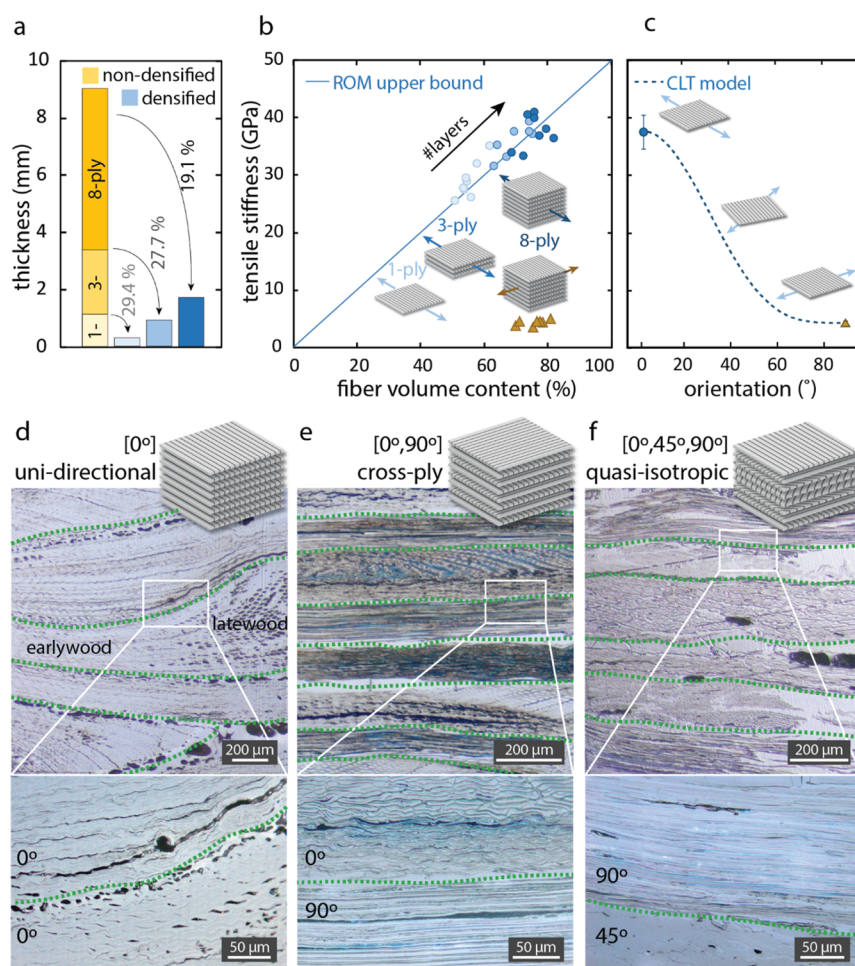


**Figure 3.** (a) Thickness of nondensified laminates compared to their densified state for one-ply, three-ply, and eight-ply unidirectional laminates. (b) Tensile stiffness vs fiber volume content of one-ply, three-ply, and eight-ply unidirectional laminates compared to the upper limit ROM demonstrate that their moduli correspond well with the bounds of theoretical prediction. (c) Tensile stiffness vs orientation according to the CLT model. (d–f) Light microscopy images of eight-ply laminates. (d) Unidirectional, (e) cross-ply, and (f) quasi-isotropic, and the zoomed in bonding line region of the corresponding laminates is also shown.

stiffness was comparable to transverse properties of flax–epoxy composites<sup>37</sup> and demonstrates that mechanical interlocking at the fiber–fiber interface can successfully compensate for the lack of a matrix. Cross-ply laminates had tensile stiffnesses of 26.7 and 17 GPa for three-ply and eight-ply laminates, respectively, and quasi-isotropic laminates showed a stiffness of 15.4 GPa. We compared these average experimental results for various laminate-stacking sequences with the theoretical predictions using the CLT model (Figure 4c). The values agree well with our CLT model calculations (see the Supporting Information), indicating that a strong bonding in between the layers is present in the cellulose–starch laminates.

The measured tensile strengths reached values between 164 and 210 MPa for unidirectional laminates (Figure 4d). Surprisingly, the tensile strength does not increase from the three-ply to the eight-ply laminate even though the FVC does. A possible explanation is the larger number of layer interfaces in the case of the eight-ply laminate, which may result in increased interface defects and thus lead to decreased strength. Quasi-isotropic laminates had slightly higher tensile strength values of 80–110 MPa compared to cross-ply laminates with a strength of 50–100 MPa, which was expected due to the higher FVC of 72% in the quasi-isotropic laminate compared to about 65% for the cross-ply laminate.

The cellulose–starch laminates possess a density of approximately 1.1 g/cm<sup>3</sup>. This is relatively low compared to matrix-containing composites of equivalent mechanical properties and thus presents a clear advantage in specific mechanical performance. A comparison of specific tensile properties with literature values is plotted in Figure 4d. Unidirectional cellulose–starch laminates performed better than bio-based flax composites<sup>6</sup> and jute<sup>38</sup> or paper-based<sup>21</sup> materials. The laminates even showed a higher specific stiffness compared to delignified densified bulk wood; however, the specific strength is lower,<sup>29</sup> possibly due to an increased number of defects at the layer–layer interface compared to the delignified densified bulk wood samples. The laminates' tensile properties are also in the range of respective values of glass fiber-reinforced epoxy composites (50% FVC).<sup>34</sup>

In addition, the beneficial effect of laminates with a parallel alignment of cellulose fibers on the material's stiffness becomes apparent by comparing the values of a recent study where high-density molded pulp fibers materials of similar porosity were fabricated. The maximum stiffness in that case was about 20 GPa, which is significantly lower than the reported properties here.<sup>39</sup> A higher strength was achieved by Soykeabkawe et al. with a surface selective dissolution of regenerated cellulose fibers followed by densification, which lead to a FVC of

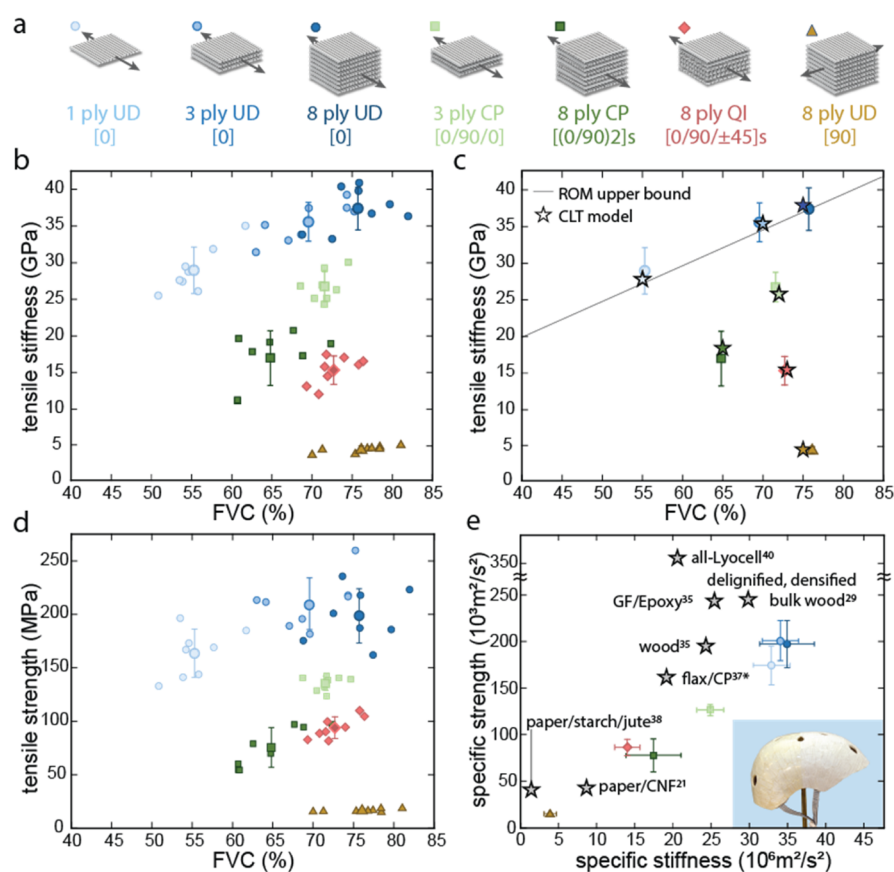


**Figure 4.** (a) Schematic illustration of the starch–cellulose laminates showing the testing condition with arrows. (b) Tensile stiffness vs FVC. (c) Average stiffness values, upper limit ROM showing the linear behavior of UD laminates and calculated values according to the CLT (stars). (d) Tensile strength of laminates and (e) specific tensile strength vs specific tensile stiffness for comparing the density-normalized properties to reference values and cellulose–starch helmet that was fabricated in a quasi-isotropic manner.<sup>30,36</sup>

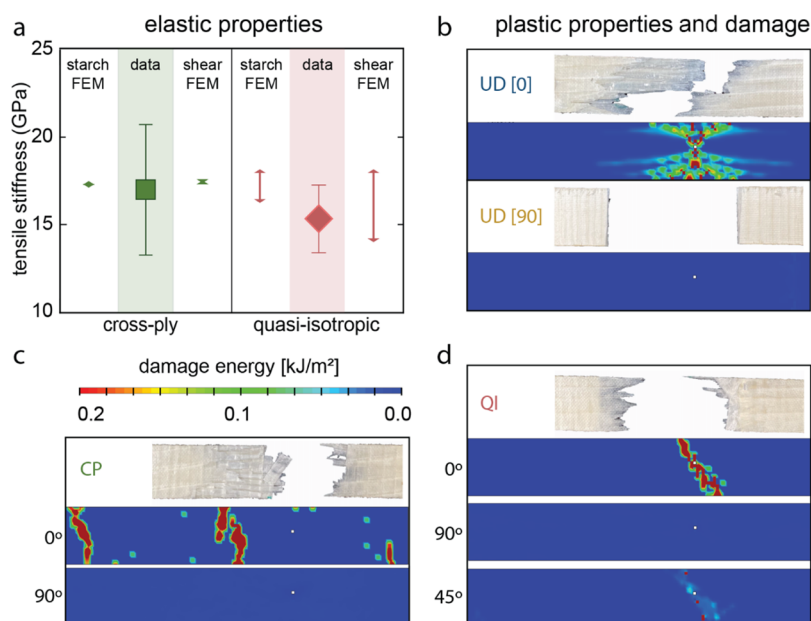


**Figure 5.** (a) Average and standard deviation of experimental data (shaded area) for eight-ply cross-ply and quasi-isotropic laminates in comparison with the tensile stiffness range predicted by the FEM by varying the starch elastic modulus between 3 and 36 GPa and the shear modulus between 1 and 7 GPa. (b–d) Fracture images of laminates of different layouts and the corresponding FEM predictions of damage energy dissipation following the failure of the specimen.

approximately 80% and very little defects in the composite.<sup>40</sup> However, the manufacturing of such regenerated cellulose-

based materials comprises many processing steps including chemicals that are less sustainable<sup>30</sup> as of present. Here, we



made a theoretical approach to look into tunable properties such as the adhesive stiffness and in-plane shear modulus on the overall mechanical performance of the composite.

We performed FEM to gain a deeper understanding of the interdependency between starch mechanical properties and single layers and its influence on the overall elastic performance of the final composite. The modeling assumed cross-ply and quasi-isotropic laminates to be constructed of single layers with adhesive interlayers of various elastic properties. This analysis showed that a large variation in the interlayer stiffness (i.e., from about 8% of the constituent layer stiffness to 100%) resulted in up to 13% change in the stiffness of a final composite (Figure 5a). Additionally, when comparing the impact of starch stiffness on the elastic behavior of eight-ply UD[0] and UD[90], we found the latter to have a similar contribution of the adhesive layer stiffness (~10%), while for UD[0] we observed no effect. This small influence on laminate stiffness despite the large change in the adhesive layer stiffness can be explained by the glue's relatively small volume fraction in the final composite.

The shear modulus of the single layer was experimentally unknown but has a significant influence on laminate stiffness. By varying the parallel to the grain shear modulus (i.e., equally varying  $G_{LT}$  and  $G_{LR}$ , Table S3) between 1 and 7 GPa, our model predicted up to a 30% increase in stiffness of quasi-isotropic laminates, while the stiffness of laminates with other stacking sequences were not affected. This suggests that an increase in the shear modulus of the single layer could substantially improve the quasi-isotropic laminate tensile properties. Apart from the elastic properties of the composites, the contribution of a given single layer on plastic deformation and damage propagation was also studied. In Figure 5b–d, individual fracture patterns for each laminate are compared for experimental and simulation results. In the unidirectional laminate, the crack is deflected, through a combination of interface damage and fiber rupture, from the normal direction of the applied stress and thus resists a load drop and contributes to a large dissipation of energy. On the contrary, the transverse specimens had straight cracks propagating purely normal to the load direction. We observed a sharp load drop corresponding to very small damage energies.

The cross-ply and quasi-isotropic laminates were both found to have complex fracture patterns. The amount of damage energy in the individual layer differs substantially for both configurations. In the cross-ply laminate, the crack deviates from being purely normal to the load direction, and a large but localized damage dissipation energy is seen in the 0° direction. In quasi-isotropic laminates, an evident 45° pattern is observed both experimentally and in the model with large damage energy at the 0° direction and considerably smaller energy dissipated at the 45° direction. These all indicate that predominant energy dissipation occurred through fiber rupture and interface damage in the 0°.

## CONCLUSIONS

Here, we report high-performance, all-bio-based composite laminates of delignified densified wood veneers and starch fabricated using a scalable and efficient wet processing. First, we investigated the ideal starch–adhesive concentration. Then, unidirectional, cross-ply, and quasi-isotropic laminates were manufactured by stacking wet delignified wood veneers and starch-/water-based interfaces. Densification was conducted using an open-mold process that is readily scalable and allows

the production of flat or shaped laminates depending on the application. The interface strategies to improve fiber bonding were inspired by well-studied methodologies used for paper, such as starch gluing or mechanical interlocking and the interlocking between neighboring fibers of delignified wood, to result in high tensile properties. For unidirectional laminates, a linear increase in stiffness with FVC was obtained reaching up to 40 GPa for an 80% FVC. The FVCs were found to depend on the number of layers and the angle between adjacent layers as well as processing conditions. Independent of the FVC, the in-plane tensile properties of cross-ply and quasi-isotropic laminates agree well with the classical laminate theory, allowing engineers to use this approach to design composites using the proposed method. Using our simulations, we highlighted the small influence of the choice of adhesive and large influence of the layer shear stiffness on the final laminate tensile stiffness.

For this first study on these new laminate composites, we focused on a detailed understanding of the tensile behavior by complementary experiments and simulations. The next important steps include mechanical tests under further types of loading, analysis regarding the material's sustainability and eco-friendliness compared to other plant-derived materials, and the improvement of the composite's performance at higher humidity levels.

The combination of wood and starch, both renewable and abundantly available resources, in an efficient and scalable manufacturing process could result in recyclable bio-based laminates that are predestined for novel bio-composite applications in dry conditions.

## ASSOCIATED CONTENT

### Supporting Information

The Supporting Information is available free of charge at <https://pubs.acs.org/doi/10.1021/acssuschemeng.0c08373>.

Mechanical properties of laminates and the corresponding densification parameters, CLT model calculations and FEM parameters, IR spectra of reference and delignified veneers, and wet chemistry analysis including the corresponding materials and methods section (PDF)

## AUTHOR INFORMATION

### Corresponding Authors

**Marion Frey** – Wood Materials Science, Institute for Building Materials, ETH Zürich, Zurich CH-8093, Switzerland; WoodTec Group, Cellulose & Wood Materials, EMPA, Dübendorf CH-8600, Switzerland; [orcid.org/0000-0002-9242-4331](https://orcid.org/0000-0002-9242-4331); Email: [marion.frey@bcomp.ch](mailto:marion.frey@bcomp.ch)

**Tobias Keplinger** – Wood Materials Science, Institute for Building Materials, ETH Zürich, Zurich CH-8093, Switzerland; WoodTec Group, Cellulose & Wood Materials, EMPA, Dübendorf CH-8600, Switzerland; [orcid.org/0000-0003-0488-6550](https://orcid.org/0000-0003-0488-6550); Email: [tkeplinger@ethz.ch](mailto:tkeplinger@ethz.ch)

### Authors

**Livia Schneider** – Wood Materials Science, Institute for Building Materials, ETH Zürich, Zurich CH-8093, Switzerland

**Hajar Razi** – Wood Materials Science, Institute for Building Materials, ETH Zürich, Zurich CH-8093, Switzerland; WoodTec Group, Cellulose & Wood Materials, EMPA, Dübendorf CH-8600, Switzerland



Etienne Trachsel – Wood Materials Science, Institute for Building Materials, ETH Zürich, Zurich CH-8093, Switzerland

Eric Faude – Wood Materials Science, Institute for Building Materials, ETH Zürich, Zurich CH-8093, Switzerland

Sophie Marie Koch – Wood Materials Science, Institute for Building Materials, ETH Zürich, Zurich CH-8093, Switzerland; WoodTec Group, Cellulose & Wood Materials, EMPA, Dübendorf CH-8600, Switzerland; [orcid.org/0000-0002-1718-4999](https://orcid.org/0000-0002-1718-4999)

Kunal Masania – Shaping Matter Lab, Faculty of Aerospace Engineering, TU Delft, HS Delft 2629, the Netherlands; [orcid.org/0000-0001-9498-1505](https://orcid.org/0000-0001-9498-1505)

Peter Fratzl – Department of Biomaterials, Max Planck Institute of Colloids and Interfaces, Potsdam 14424, Germany

Ingo Burgert – Wood Materials Science, Institute for Building Materials, ETH Zürich, Zurich CH-8093, Switzerland; WoodTec Group, Cellulose & Wood Materials, EMPA, Dübendorf CH-8600, Switzerland; [orcid.org/0000-0003-0028-072X](https://orcid.org/0000-0003-0028-072X)

Complete contact information is available at:  
<https://pubs.acs.org/10.1021/acssuschemeng.0c08373>

## Author Contributions

M.F., H.R., L.S., E.T., E.F., and S.M.K.: Performed experiments and analyzed data. M.F., K.M., H.R., P.F., T.K., and I.B.: Analyzed data and co-wrote the manuscript.

## Funding

This work was financed in the framework of the project “Strong Composite” supported under the umbrella of ERANET Cofund ForestValue by Innosuisse, AKA, Business Finland, Vinnova, BMLFUW. ForestValue received funding from the European Union’s Horizon 2020 research and innovation program under grant agreement 773324. HR acknowledges funding from the European Union’s Horizon 2020 research and innovation program under the Marie Skłodowska-Curie grant agreement number 754364.

## Notes

The authors declare no competing financial interest.

## ACKNOWLEDGMENTS

The authors would like to thank Thomas Schnider for the preparation of the wood samples, Günther Gratzl from Agrana for kindly supplying the starch-based glue, Meri Zirkelbach for providing the helmet picture in Figure 4, Silvan Gantenbein for 3D-printing of molds, Kunkun Tu for help with illustrations, and the Scientific Center for Optical and Electron Microscopy (ScopeM) of ETH for providing the SEM instrument, the ultramicrotome, and technical support.

## REFERENCES

- (1) Mohanty, A. K.; Misra, M.; Drzal, L. T. Sustainable biocomposites from renewable resources: opportunities and challenges in the green materials world. *J. Polym. Environ.* **2002**, *10*, 19–26.
- (2) Huda, M. S.; Drzal, L. T.; Ray, D.; Mohanty, A. K.; Mishra, M. *Properties and Performance of Natural-Fibre Composites*; Pickering, K. L., Ed.; Woodhead Publishing, 2008; pp 221–268.
- (3) Mohanty, A. K.; Vivekanandhan, S.; Pin, J.-M.; Misra, M. Composites from renewable and sustainable resources: Challenges and innovations. *Science* **2018**, *362*, 536–542.

- (4) Koronis, G.; Silva, A.; Fontul, M. Green composites: a review of adequate materials for automotive applications. *Composites, Part B* **2013**, *44*, 120–127.
- (5) Huber, T.; et al. A critical review of all-cellulose composites. *J. Mater. Sci.* **2012**, *47*, 1171–1186.
- (6) Woigk, W.; et al. Fabrication of flax fibre-reinforced cellulose propionate thermoplastic composites. *Compos. Sci. Technol.* **2019**, *183*, 107791.
- (7) Hottle, T. A.; Bilec, M. M.; Landis, A. E. Sustainability assessments of bio-based polymers. *Polym. Degrad. Stab.* **2013**, *98*, 1898–1907.
- (8) Sakurada, I.; Nukushina, Y.; Ito, T. Experimental determination of the elastic modulus of crystalline regions in oriented polymers. *J. Polym. Sci.* **1962**, *57*, 651–660.
- (9) Nishino, T.; Takano, K.; Nakamae, K. Elastic modulus of the crystalline regions of cellulose polymorphs. *J. Polym. Sci., Part B: Polym. Phys.* **1995**, *33*, 1647–1651.
- (10) Rowell, R. M. *Handbook of Wood Chemistry and Wood Composites*; CRC Press: Boca Raton, 2012.
- (11) Speck, T.; Burgert, I. Plant stems: functional design and mechanics. *Annu. Rev. Mater. Res.* **2011**, *41*, 169–193.
- (12) Gibson, L. J. The hierarchical structure and mechanics of plant materials. *J. R. Soc. Interface* **2012**, *9*, 2749–2766.
- (13) Fortea-Verdejo, M.; Bumbaris, E.; Burgstaller, C.; Bismarck, A.; Lee, K.-Y. Plant fibre-reinforced polymers: where do we stand in terms of tensile properties? *Int. Mater. Rev.* **2017**, *62*, 441–464.
- (14) Pickering, K. L.; Efendy, M. G. A.; Le, T. M. A review of recent developments in natural fibre composites and their mechanical performance. *Composites, Part A* **2016**, *83*, 98–112.
- (15) Schmied, F. J.; et al. What holds paper together: Nanometre scale exploration of bonding between paper fibres. *Sci. Rep.* **2013**, *3*, 2432.
- (16) Vainio, A.; Paulapuro, H. Interfiber bonding and fiber segment activation in paper. *BioResources* **2007**, *2*, 442–458.
- (17) Tanaka, A.; Niskanen, K.; Hiltunen, E. J.; Kettunen, H. Inter-fiber bonding effects of beating, starch or filler. *Nord. Pulp Pap. Res. J.* **2001**, *16*, 306–312.
- (18) Taipale, T.; Österberg, M.; Nykänen, A.; Ruokolainen, J.; Laine, J. Effect of microfibrillated cellulose and fines on the drainage of kraft pulp suspension and paper strength. *Cellulose* **2010**, *17*, 1005–1020.
- (19) Reynolds, W. F. *Dry strength additives: a project of the Papermaking Additives Committee*; Tappi Pr, 1980; Vol. 44.
- (20) Hubbe, M. Bonding between cellulosic fibers in the absence and presence of dry-strength agents—A review. *BioResources* **2006**, *1*, 281–318.
- (21) Yousefi Shivyari, N.; Tajvidi, M.; Bousfield, D. W.; Gardner, D. J. Production and characterization of laminates of paper and cellulose nanofibrils. *ACS Appl. Mater. Interfaces* **2016**, *8*, 25520–25528.
- (22) Scholz, R.; Langhansl, M.; Zollfrank, C.; Walther, F. Experimental study on the actuation and fatigue behavior of the biopolymeric material Cottonid. *Mater. Today: Proc.* **2019**, *7*, 476–483.
- (23) Jeronimidis, G.. In *Structural biological materials—Design and structure-property relationships*; Elices, M., Ed.; Pergamon Materials Series; Pergamon: Kidlington, 2000; pp 19–29.
- (24) Naleway, S. E.; Porter, M. M.; McKittrick, J.; Meyers, M. A. Structural design elements in biological materials: application to bioinspiration. *Adv. Mater.* **2015**, *27*, S455–S476.
- (25) Berglund, L. A.; Burgert, I. Bioinspired Wood Nanotechnology for Functional Materials. *Adv. Mater.* **2018**, *30*, 1704285.
- (26) Yano, H. Potential strength for resin-impregnated compressed wood. *J. Mater. Sci. Lett.* **2001**, *20*, 1127–1129.
- (27) Keplinger, T.; Wang, X.; Burgert, I. Nanofibrillated cellulose composites and wood derived scaffolds for functional materials. *J. Mater. Chem. A* **2019**, *7*, 2981–2992.
- (28) Fu, Q.; Ansari, F.; Zhou, Q.; BerglundWood, L. Nano-technology for Strong, Mesoporous, and Hydrophobic Biocomposites for Selective Separation of Oil/Water Mixtures. *ACS Nano* **2018**, *12*, 2222–2230.

- (29) Frey, M.; et al. Delignified and Densified Cellulose Bulk Materials with Excellent Tensile Properties for Sustainable Engineering. *ACS Appl. Mater. Interfaces* **2018**, *10*, 5030–5037.
- (30) Frey, M.; et al. Fabrication and Design of Wood-Based High-Performance Composites. *JoVE* **2019**, *153*, No. e60327.
- (31) Maurer, H. W. Starch in the Paper Industry BeMiller, J., Whistler, R., Eds.; 3rd ed.; Academic Press: New York, 2009, pp 657–713.
- (32) Stoeckel, F.; Konnerth, J.; Gindl-Altmutter, W. Mechanical properties of adhesives for bonding wood—A review. *Int. J. Adhes. Adhes.* **2013**, *45*, 32–41.
- (33) Hirn, U.; Schennach, R. Comprehensive analysis of individual pulp fiber bonds quantifies the mechanisms of fiber bonding in paper. *Sci. Rep.* **2015**, *5*, 10503.
- (34) Frey, M.; et al. Tunable Wood by Reversible Interlocking and Bioinspired Mechanical Gradients. *Adv. Sci* **2019**, *6*, 1802190.
- (35) Frey, M.; Schneider, L.; Masania, K.; Keplinger, T.; Burgert, I. Delignified wood-polymer interpenetrating composites exceeding the rule of mixtures. *ACS Appl. Mater. Interfaces* **2019**, *11*, 35305–35311.
- (36) <https://www.empa.ch/de/web/s604/holz-paradox-eq66> accessed December 2020.
- (37) Woigk, W.; et al. Interface properties and their effect on the mechanical performance of flax fibre thermoplastic composites. *Composites, Part A* **2019**, *122*, 8–17.
- (38) Verma, B. B. Continuous jute fibre reinforced laminated paper composite and reinforcement-fibre free paper laminate. *Bull. Mater. Sci.* **2009**, *32*, 589–595.
- (39) Yang, X.; Berthold, F.; Berglund, L. A. High-Density Molded Cellulose Fibers and Transparent Biocomposites Based on Oriented Holocellulose. *ACS Appl. Mater. Interfaces* **2019**, *11*, 10310–10319.
- (40) Soykeabkaew, N.; Nishino, T.; Peijs, T. All-cellulose composites of regenerated cellulose fibres by surface selective dissolution. *Composites, Part A* **2009**, *40*, 321–328.